

AD-A152 806



AIR PRODUCTS

R&D STATUS REPORT

DARPA ORDER NO.: 4746

PROGRAM CODE NO.: --

CONTRACTOR: Air Products and Chemicals, Inc.

CONTRACT NO.: N00014-83-C-0394

10NR

CONTRACT AMOUNT: \$594,000

EFFECTIVE DATE OF CONTRACT: '83 July 01

EXPIRATION OF CONTRACT: '85 September 30

PRINCIPAL INVESTIGATOR: W. A. Steyert

PHONE NO.: (215) 481-3700

PROGRAM MANAGER: R. C. Longworth

PHONE NO.: (215) 481-3708

SHORT TITLE OF WORK: Solid State Compressor

REPORTING PERIOD: '84 October 01 - '84 December 31

o PROGRESS:

Progress Report is attached.

o KEY PERSONNEL: No changes

o SPECIAL EVENTS: None

o PROBLEMS ENCOUNTERED AND/OR ANTICIPATED: We are continuing to experience a delay in getting the ceramic drivers from our subcontractor, Pennsylvania State University.

DTIC
ELECTE
APR 25 1985
S D A

FISCAL STATUS:

- (1) Amount currently provided on contract:
- (2) Expenditure and commitments to date: Per separate report
- (3) Funds required to complete work: Per contract

CLEARED
FOR OPEN PUBLICATION

APR 23 1985 19

REVIEW OF THIS MATERIAL DOES NOT IMPLY
DEPARTMENT OF DEFENSE INDORSEMENT OF
FACTUAL ACCURACY OR OPINION.

DIRECTORATE FOR FREEDOM OF INFORMATION
AND SECURITY REVIEW (OASD-PA)
DEPARTMENT OF DEFENSE

-1- APPROVED FOR PUBLIC RELEASE
DISTRIBUTION IS UNLIMITED (A)

0 1535

DTIC FILE COPY

1.0 SUMMARY

Pennsylvania State University has continued their basic ceramic material studies but has been unable to fabricate complete high performance drivers.

APCI continued testing and modifying the one cell simulator. Work was also done on fabricating elastomers and designing a one cell prototype compressor.

CeramPhysics analyzed the drive characteristics of the three cell simulator and achieved a 2:1 compression ratio with the peristaltic compression mechanism.

We believe that the single cell prototype compressor which is being designed will demonstrate the feasibility of building a closed cycle J-T compressor which incorporates the "solid state compressor" concepts.

Accession For	
NTIS GRA&I	<input checked="" type="checkbox"/>
DTIC TAB	<input type="checkbox"/>
Unannounced	<input type="checkbox"/>
Justification	
By	
Distribution/	
Availability Codes	
Dist	Avail and/or Special
A-1	



2.0 TASK 1 DRIVERS

Pennsylvania State University has continued their basic research work on improving the characteristics of electrostrictive actuators. Their work is reported in Appendix A.

As a result of their attempts to build actuators that advance the state of the art, they have encountered difficulties in providing drivers for the prototype units. In discussing the problem with PSU, it has been decided to design the prototype compressors in such a way that they can utilize drivers which PSU can comfortably fabricate.

3.0 TASK 2.1 ONE CELL SIMULATOR

As previously discussed, the one cell simulator with an annular radial compression chamber showed good performance providing compression ratios as high as 15:1 (see Figure 2 of R&D Status Report No. 5). It suffered from leaks in the seal between the elastomer and the body of the compressor. Two new compressor elastomer force plate assemblies were built. The elastomer of one unit was 20 durometer Monothane (from Endpol Corporation). The other elastomer was Ecco Gel 1365-0 (from Emerson Cummings). These were built with help from Professor James Runt, consultant from Penn State. The Ecco Gel assembly was glued into the compressor body. It is leak tight. It will be tested as soon as the new simulator components with a linear motion transducer are prepared, Figure 1.

Attempts were made to use low durometer Silastic in the one cell simulator. It is very soft and has a high tear strength for a low durometer material. In addition, it has a low glass transition temperature so that, by Visco elastic theory, it will not have a large modulus increase as temperature drops or operating frequency increases. Unfortunately, we were unable to bond it to the body as is required for the currently designed compressor.

Figure 2 shows a second annular face compression chamber and a new motion amplifier concept that will be tested in the single cell simulator. The motion amplifier consists of a metal diaphragm which acts against a low durometer elastomer that extrudes into the compression space. A polyurethane sheet separates the gas from the soft elastomer. This design concept looks attractive for the prototype unit which is described in Section 7 of this report.

4.0 TASK 2.2 THREE CELL SIMULATOR

The three cell simulator was received by CeramPhysics from Air Products and Chemicals (APCI) the end of October. The simulator was designed by CPI and APCI and constructed by APCI. Two elastomer type heads for testing were supplied to CPI by APCI: (1) a tube design (Head No. 2), and (2) a membrane design (Head No. 3). All testing done to date has been on Head No. 3, ref. Figure-6, R&D Status Report No. 5.

4.1 Setup of the Three Cell Simulator

Several auxiliary parts have been added by CPI. First, a noise reduction/operator-protection box was designed and constructed for containment of the model. This box is approximately 24" x 20" x 11" with 3/4" wood walls lined with 3/4" Styrofoam noise-reducing insulation. The box is mounted with an air circulation fan, has several small holes for air flow, electrical and electronic sensor access, and gas inlet-outlet access. The box acts as a supporting frame for sensor terminations and for the gas handling plumbing.

A speed control was assembled for the simulator motor. This consists of a Dayton Electric 4X796B 5 amp motor speed control module mounted in a box with an on-off switch and a fuse. This assembly allows adjustment of the model motor speed from 0-8000 rpm.

Inlet and outlet plumbing were added to the compressor. The inlet consists of a 1/4" copper tube, valved, which is stepped down to a 1/16" stainless steel tube that enters the simulator head. The outlet from the head is a 1/16" stainless steel tube that is stepped up to a short length of 1/4" copper tube. This in turn enters a small, cylindrical "surge tank" approximately 3" long x 2" diameter (interior dimensions). Two short 1/4" copper tubes lead from the surge tank. One of these is simply a valved outlet line. The other leads to an adjustable relief valve (approximately 150 psi), which is isolated from the surge tank by a shut-off valve included for purposes of leak checking or operation above the pressure of the relief valve.

Both the inlet line and the surge tank have been instrumented with electronic pressure transducers. The inlet line utilizes an Omega Engineering Model 236PC sensor, 0-100 psig, and the outlet an Omega Engineering Model PX300 sensor, 0-500 psig. The sensitivity of the former device is 1.6 mV/psi and the latter 0.06 mV/psi.

The force members for the compression/valving pistons were outfitted with Sensotec, Inc., Model 30 force transducers. All three of these transducers are designed for 0-50 pound operation and have a sensitivity of about 0.57 mV/pound force. They are linear devices, reversible between tension and compression forces so that tension forces output positive voltages and compression forces output negative voltages. The actual sensitivities of these devices are given in Table I.

TABLE 1

<u>Cell No.</u>	<u>Sensor No.</u>	<u>Output at 50 Pounds</u>
1 output	119027	28.564 mV
2 compression	119025	29.029 mV
3 inlet	110706	27.510 mV

The cam shaft of the simulator was outfitted by APCI with Sylvania ECG 3101 opto-coupled interrupter module and a circular mask containing a

small hole. Per every rotation of the cam shaft, the hole sweeps in front of the LED of the module allowing light to fall upon a receptor in the module. This produces a timing signal from the opto-coupler which may be observed on an oscilloscope.

This opto-coupler mask was inscribed with degree markings space 10° apart. The markings have been very useful in some of the measurements described below.

All of the sensors were tied into terminal blocks, which were further wired with various leads for connection to reading instruments and to a 10 volt power supply. Sensor readings are made with Keithley Model 181 digital nanovoltmeters, a Hewlett-Packard Model 3480A DVM, and a B&K Model 1480.40 MHz oscilloscope. The power supply is a Hewlett-Packard Model 723A dc variable power supply. During some measurements, readings from the Keithley DVM's are taken automatically using an IEEE 488 interface to a Digital Equipment Pro-350 computer.

4.2 Characterization of the Cams and Cam Shaft

Since the precise shape of the individual cams and the positioning of the cams relative to one another are critical to the operation of the simulator, an effort has been made to measure the shape of the cams directly and indirectly.

The cam shaft was mounted in a lathe and an indicator was mounted rigidly to the tool carrier of the lathe in an effort to measure the rise and fall of the cams, and to measure any bend in the cam shaft. Certain aspects of these measurements were crude, e.g., the cam shaft was not precisely parallel to the axis of the lathe rotation. However, it was possible to make approximate corrections, and the results do cross-correlate with other measurements. We believe from the measurements made that the cam shaft is straight to < 1 mil, and that the cams are cut essentially correctly but not precisely to specification.

The results of the cam direct measurements are shown in Figure 3. The indicator was not changed in zero point from cam to cam; the lathe head was rotated by hand and angles were read from angle inscriptions on the chuck. The scale on this figure has been expanded to 600° rather than 360° to clearly show the shapes and relative rising-falling of the cams. Cam No. 1 is shown in circles, Cam No. 2 in triangles and Cam No. 3 in squares. The design specification is shown as a solid line curve in the center of the graph and is included for comparison purposes.

Certain trends and features may be noted in Figure 3. All three cams seem to satisfy the general shape of the compressed cycloid design. Also, the cams do seem to rise and fall in the specified 120° phasing. There is some question whether perhaps the "dwell" is about 20° longer than designed and whether the rise height is the same for all three cams. Unquestionably, the three cams do not "plateau" in the proper manner, but rather reach a peak rise 100° after the "low point" and then gradually drop in rise for about 180° . This latter effect may be visually observed when the simulator is assembled without return springs on the force members. For each cam one may rotate the cam to the "low point" (marked by a set pin in the cam through the shaft) and push the cam follower against the cam. By slowly rotating the cam shaft, the motion of the force member and the cam follower bearing may be observed then. The force member is observed to reach maximum displacement between 90° and 110° beyond the "low point," and the cam follower will retain contact with the cam and rotate (with the help of an oil film) for 40° to 80° . Beyond this, however, the cam follower and the cam are seen to separate.

4.3 Force Member Adjustment and Procedure for Setup

The adjustments of the turnbuckles (i.e., the length) of the force member/piston assemblies on the simulator are absolutely critical. One may easily imagine the extremes of the problem: If a force member is too short, not enough force will be exerted on a given cell to close it even at maximum throw of the cam. Similarly, if the force member was too small, such that a large force is applied even at minimum throw of the cam, a cell will

remain closed for all cam angle and the force member will be attempting to compress the "incompressible" elastic components of the system--a situation that would put a tremendous strain on the motor. Clearly, there is a fine dividing line between these cases, a problem which is multiplied by 3 due to the three cells. In fact, solution would be trivial if the system consisted of a single cell: one would merely establish a gas flow through the system, put the cam on "high point" and adjust the turnbuckle until gas flow barely stops. This unfortunately does not suffice when there are three cells, each with different phase relationships to each other and which should as a group be sealed at all angles. Further, due to the vagaries of this simulator design, at least for head design No. 3, there are further complicating factors that make solution tortuous.

Several studies have been made of the behavior of the valving actions of single cells on this system, and these studies have been combined in several attempted strategies for adjustment of the cells. Unfortunately, it seems that there is no easily quantifiable (reproducible) methodology; rather, setup is a rather empirical "chance" matter.

The head No. 3 design is shown in representative cross section in Figure 4. From this figure it may be seen that 10 mil polyurethane sheet is used as the gas seal over an interconnected system of three milled out depressions in the head. Interposed between the pistons and the depressions are disks of 1/4" zero durometer neoprene. The first and third depressions, acting as inlet and outlet valves, are smaller than the second depression, which is to act as the main pumping cell. The surface areas of these three depressions are all quite large, approximately 0.31 in² and 0.98 in², respectively. The pistons are larger than the depressed areas in cross section: 0.36 in² and 1.47 in², respectively. Intuition indicated that the behavior force observed exerted by a force member versus turnbuckle setting would appear as in Figure 5. That is, the force would remain essentially a low constant until the piston contacted the neoprene disk, would begin an upward curve as the neoprene was "squashed" into the depression in the head and then would rise sharply

upward as force is applied to "compression" of the neoprene. Intuition also indicated that the "dwell" of this arrangement, i.e., the angle through which gas flow would be cut off by a single cell, would be subject to several variables, e.g., inlet pressure, back flow pressure, and turnbuckle setting (maximum/minimum force applied by the piston). A number of experiments were conducted on each of the single cells to investigate these conjectures.

In one set of experiments all of the turnbuckles were turned to give minimum push rod length; then, choosing one of the three cam/rod assemblies, the cam shaft was rotated until the particular cam was 180° from its low point. A flow of helium gas was established through the system using a tank supply regulated to a low pressure and indicated by bubbling the outlet through a beaker of water. The turnbuckle was then turned and force cell readings were taken. In this manner the behavior sketched qualitatively in Figure 5 was established as essentially correct. The valve cells shut off in the upturn region after the knee, as anticipated; but the force required was rather unclear since small turns of the turnbuckles resulted in large changes in the force applied. The quantitative behavior of the system and flows observed in this manner did not seem particularly reproducible, and the force required in a given cell to shut off the flow was found to depend upon inlet pressure. Once approximate force values were found for shut off of the inlet and compression cells (the outlet was assumed the same as the inlet), the system turnbuckles were adjusted to apply the forces measured as above, and an attempt was made to run the system. No flow was observed until the inlet and outlet cells were readjusted to an arbitrarily determined lower force, but the experiment at that time was inconclusive whether the flow was a pumping action of the compressor or the result of the 10 psig input pressure that was used.

The experiments did not reveal information regarding the effective dwell of any of the cells; thus another procedure was attempted. All of the push rods were backed off to allow free flow through the system. For each turnbuckle/push rod assembly with the cam for that assembly at true

"high point" (approximately 110° from true low point), the turnbuckle/inlet pressure was adjusted until there was no flow with a 10 psig inlet pressure of helium. The cam shaft was then turned by 10° increments for all angles where no flow occurred, and the readings of the load cell were recorded. The turnbuckle was then adjusted a small amount, and the procedure of "mapping" was repeated. The results of this procedure are graphed in Figures 6 to 8. The circular data points represent a turnbuckle setting $1/16$ greater than that of square points and $1/8$ greater than that of the triangular points. The data shown are data gathered only for those angles where no flow was observed.

A number of points may be made from this experiment. One may note from the figures that the cam shapes found in Figure 3 are confirmed--there is a slight drop in cam height most noticeable in Cams 1 and 3 in the region where cam height is supposed to be a constant high. Cam 2 is indicated in the load cell readings to have more of a dip than a drop-off, as seen in Figure 3. In fact, at one turnbuckle setting (designated by triangles), flow appeared for a time (dotted lines) while the cam was turned to this dip and was stopped when the cam reached its "second highest" point.

The effective dwell of any given cell depends upon the setting of the turnbuckle but in a "breakpoint" manner. For Cam No. 1, for example, $1/16$ of a turn of the turnbuckle resulted in a change of effective dwell from 210° to 80° . But for most of the other cases, regardless of the setting, the effective dwell for single cells was approximately 240° . This is right at the allowable limit for dwell in a 120° phased system, beyond which pumping action is hypothetically impossible.

The plot for Cam No. 2 demonstrates that particular turnbuckle settings do not necessarily lead to reproducible forces: note that the turnbuckle setting supposedly $1/8$ turn "less" than the highest force setting is higher in measured forces than the $1/16$ turn "less" case. Also note that though the measured forces at all angles were higher than the $1/16$ case, the sealing characteristics of this setting were worse.

Assuming a mean dwell of 200°, the cell-filling characteristics can be represented graphically, and this is shown in Figure 9. This representation demonstrates that gas is moved from left to right.

In recent tests a 2:1 compression ratio was achieved (between the inlet pressure and the surge tank pressure), but the surge tank pressure leveled off at this value. This was traced using a leak detector to various leaks including a leak between the polyurethane sheet and the metal flat of the head; that is in Cell 2 the edge of the sheet is too close to the edge of the piston cylinder so that the covering metal block cannot adequately seal off the depression. Various attempts were made to effect a better seal using greases and a second sheet, but to no avail.

In early tests it was observed that the motor stalled even at high rpm's. This was traced to an overloading of the motor shaft. In the original construction oil lubricated metal sleeves were used in the shaft mounting brackets which galled when they ran dry. Thus, the motor overload was due to metal-on-metal bearing surfaces. The bellows coupling was modified; rotary ball bearings were installed, and the problem was solved. In addition, the return springs were installed, and the motor could be run without stalling over the full rpm design range.

A chronic problem has been the failure of the cam-follower bearings. More rugged, compatible bearings have been ordered and received.

4.4 Future Plans

Most of the bugs in the simulator have been worked out, except for the leak in Cell No. 2 which will have to be lived with. The test facility is fully instrumented, including interfacing with the computer.

The test procedure now is to "tinker" with the simulator to obtain compression ratios in the range 3:1 to 4:1, and once obtained, to measure

the pressure buildup in the surge tank with time for various inlet pressures and motor speeds.

After these tests are completed, CPI will begin testing Head No. 2.

5.0 TASK 3 DRIVER ELECTRONICS

No work has been done thus far on the driver electronics. The prototype units can be driven with standard power amplifiers. Once the characteristics of the driver ceramics are known, then special electronic units can be designed which will recover much of the energy that is used to charge a driver and thus operate more efficiently.

6.0 SYSTEM ANALYSIS

The "NIKE 2D" and "NIKE 3D" programs were purchased by APCI from Lawrence Livermore Labs and have been put into operational status. They are very powerful programs for analyzing stress-strain relations in elastomers, axisymmetric geometries or arbitrary three-dimension geometries. They will be used to analyze the stress in the elastomer in the prototype unit.

7.0 TASK 4.2 PROTOTYPE SINGLE CELL COMPRESSOR

We are expecting to get electrostrictive ceramic actuators from Penn State in the near future. A single cell compressor is being designed to use these actuators when they are prepared. Because the initial ceramics will not be able to generate the force and to provide the motion that the final actuators will need, we have decided to use a number of ceramics in parallel to get the required force and motion. Figure 10 shows the design.

The design is based on our experience with the single cell and three cell simulators. It uses a low durometer elastomer which serves as the motion amplifier; however, rather than rely on a glued joint for a pressure seal, a polyurethane diaphragm is used. This diaphragm is abrasion resistant and nonpermeable. The low durometer elastomer is not required to slide anywhere. The thin section of the metal cap on the bottom of the elastomer bends to compress the elastomer.

The gas that is compressed in each stage can flow through a short tube to the next compression stage, arranged head to head in a multicell unit. Thus, we use the peristaltic compression action without the need for valves between each stage.

We can briefly outline the analysis required to select the dimensions of the unit shown in Figure 10.

Interconnecting Hole. We take each hole to be 1/2" long between stages. If the hole is taken as 0.024" (0.61 mm) in diameter, then the clearance volume in each stage of compression (1" of hole) is $7.6 \times 10^{-3} \text{ cm}^3$. This is small compared to the 0.26 cm^3 compressor displacement (see Eq. 1 to follow).

Actuator Properties. We are planning for actuators which can provide a strain of 10^{-3} with an applied field of roughly 20,000 V/cm. We also expect a pressure of about 5,100 psi to be available if the field is applied to a clamped ceramic. The compressor is sized so that when the electric field is applied to the ceramic, the pressure generated is half the clamped value and the strain is half of the free strain. This extracts the maximum work from the ceramic. Figure 11 shows that motion ΔL of the metal cap will be $12 \times (1/2 \times 10^{-3}) = .006$ ". The available force will be $2,550 \text{ psi} \times 0.2 \text{ sq. in.} = 510 \text{ lb.}$ for two drivers.

Metal Cap Design. This results in a compressor of displacement.

$$V = \frac{\pi}{12} \Delta L (D^2 + dD + d^2) = 0.26 \text{ cm}^3 \quad (1)$$

where D and d are 2.25 and 1.50 inches, respectively. We have taken the deformation of the cap to be that of a truncated cone. If we take the compressor to have a gas at 2 atm absolute entering, and compress it by a factor of 5 in this stage, we will require the metal cap to supply a pressure of 10 atm to the elastomer. This requires a force of

$$F = \frac{\pi}{12} (D^2 + dD + d^2) P = 390 \text{ lb} \quad (2)$$

This is less than that available from the ceramics; there is a little force left over to cover losses.

Flexing Region Design. The flexing metal must be designed such that the force required to flex the metal is small compared to the gas compression force. Also, we must not exceed the metal's endurance limit. In addition, the bowing of the metal due to the pressure on the elastomer must represent a small volume compared to the compressor displacement, D, of 0.26 cm³.

The force required to flex the metal cap 0.003" above and below its neutral position is calculated from Case 1f of "Formulas for Stress and Strain," Fifth Edition, R. J. Roark and W. C. Young, McGraw Hill. The force is 46.2 lb-small compared to the 510 lb. available from the ceramics.

How much is metal stretched? Stress on the metal because of its deformation can be calculated from Case 1f of Roark as 4.1×10^4 psi. The endurance limit for spring steel is 9×10^4 psi (from Roark). Some Sandvik spring steels have an endurance limit of around 1.3×10^5 psi. In addition, there will be a stress of 2.5×10^4 psi associated with the elastomer, at 10 atm pressure, bowing the flexing region of the metal by 0.001". This sag represents a 0.0087 cm³ loss in compressor displacement.

The flexing member has a small safety margin in terms of endurance limit of the metal.

Elastomer. Using Eq. 17 of the January 1984 report on this project, we can calculate the force required to compress the central elastomer disk of diameter $D_1 = 1.32$ inches is only 3.3 lb. We have taken the elastic modulus of the elastomer as 300 psi. The elastomer which acts as a motion amplifier is seen to contribute only a small amount to the force load on the driver.

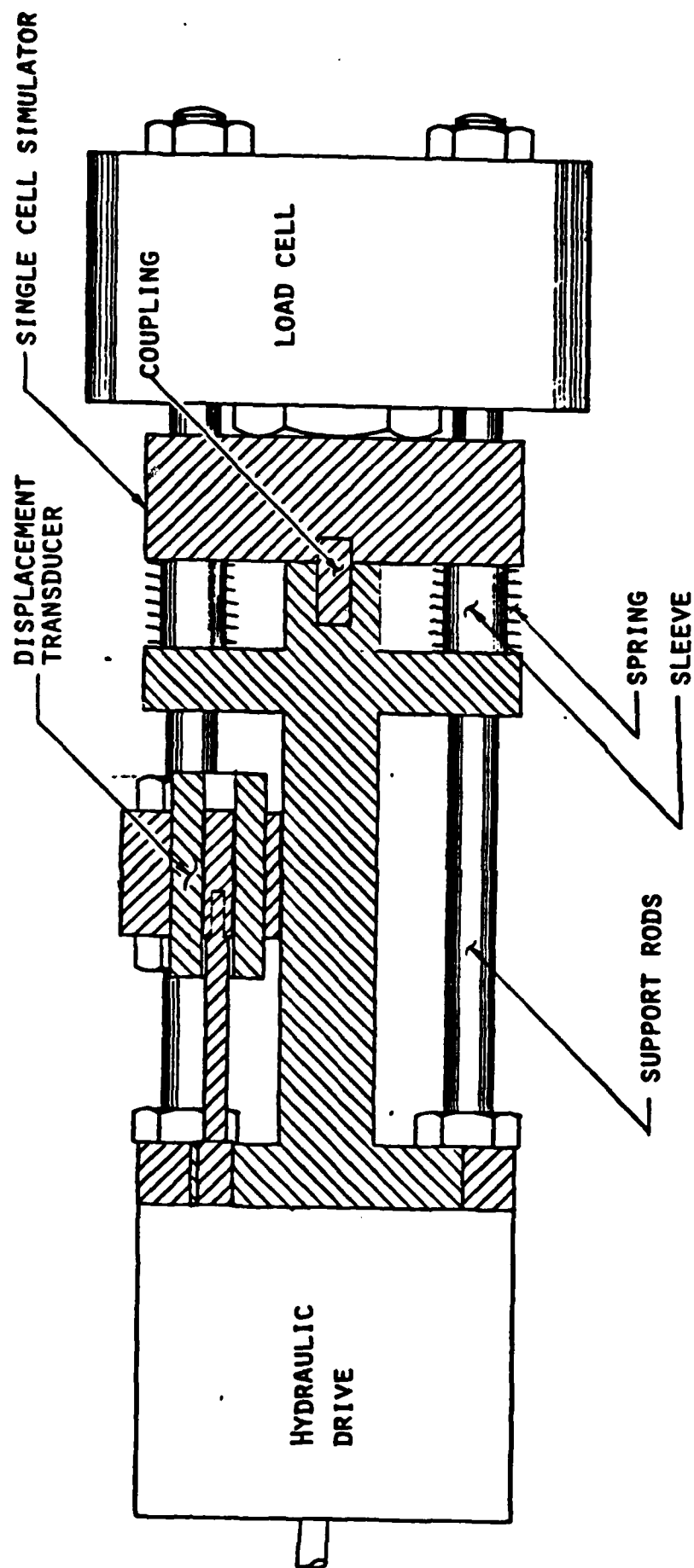


FIGURE 1. LOAD CELL AND DISPLACEMENT TRANSDUCER
MOUNT FOR SINGLE CELL SIMULATOR

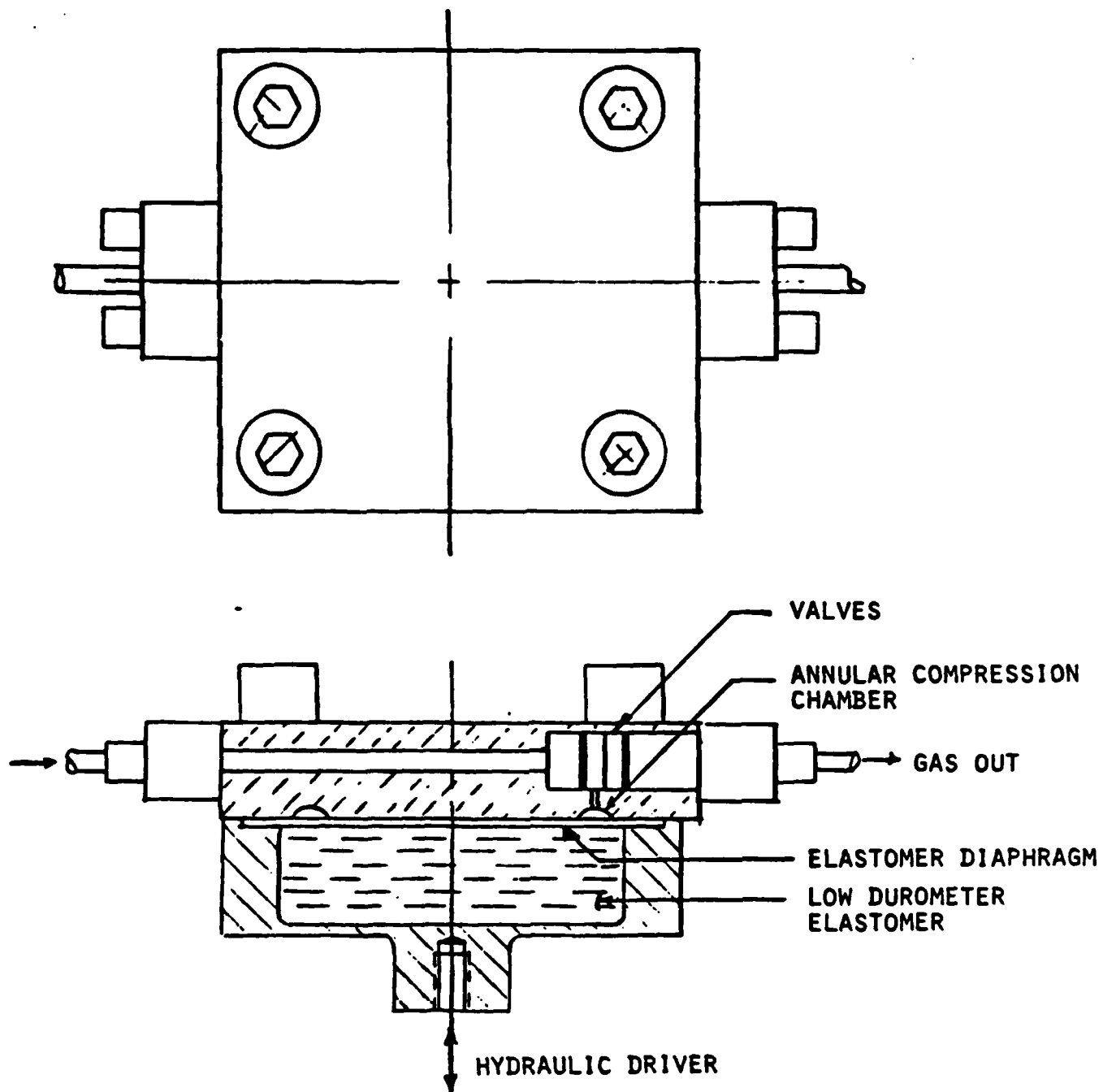


FIGURE 2. SINGLE CELL SIMULATOR, ANNULAR FACE COMPRESSION CHAMBER

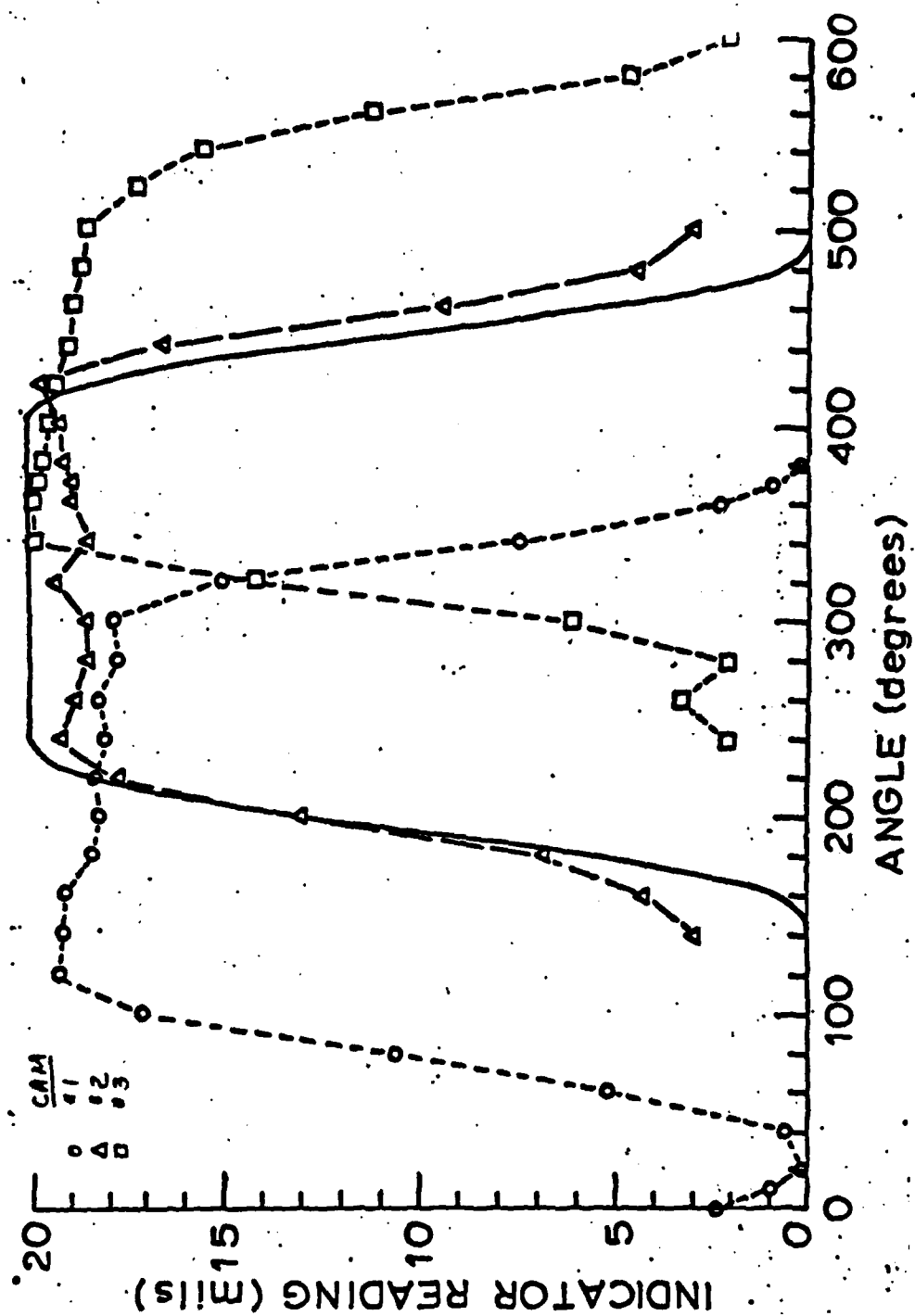


FIGURE 3. THREE CELL SIMULATOR CAM DISPLACEMENT VS. ANGLE

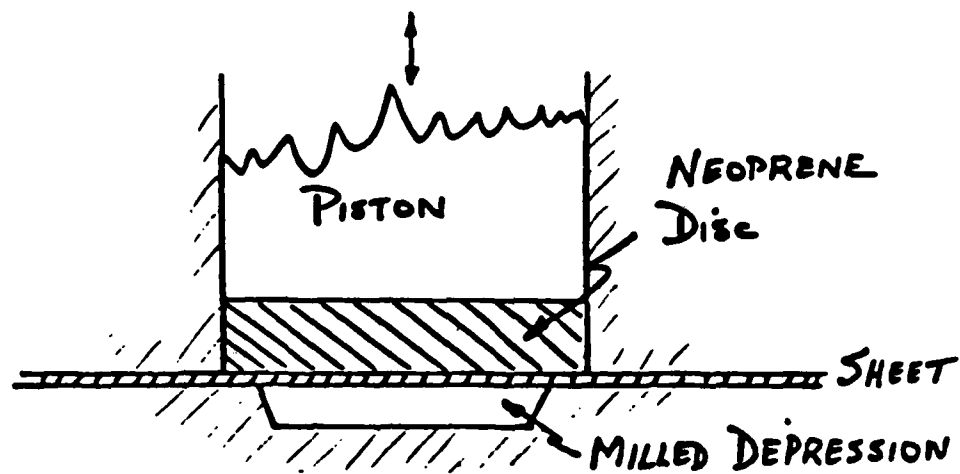


FIGURE 4. COMPRESSION CHAMBER CONSTRUCTION

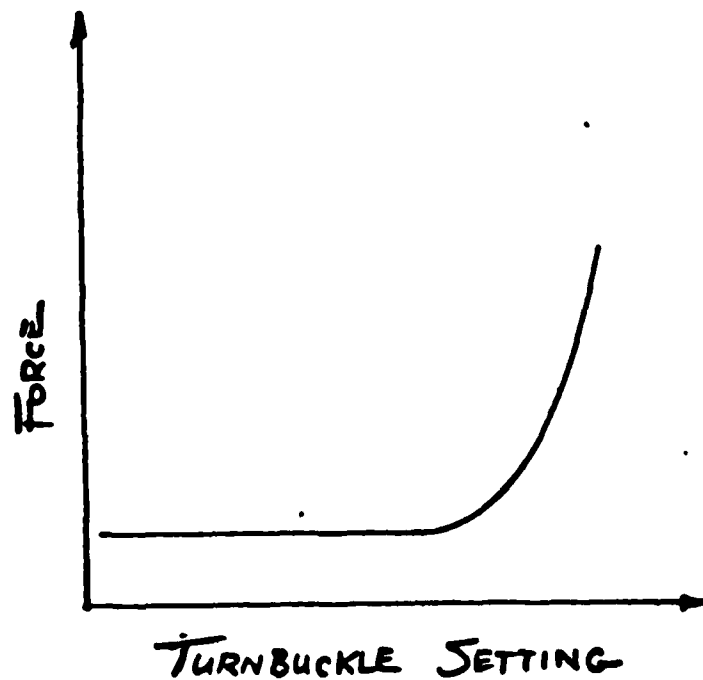


FIGURE 5. FORCE VS. TURNBUCKLE SETTING

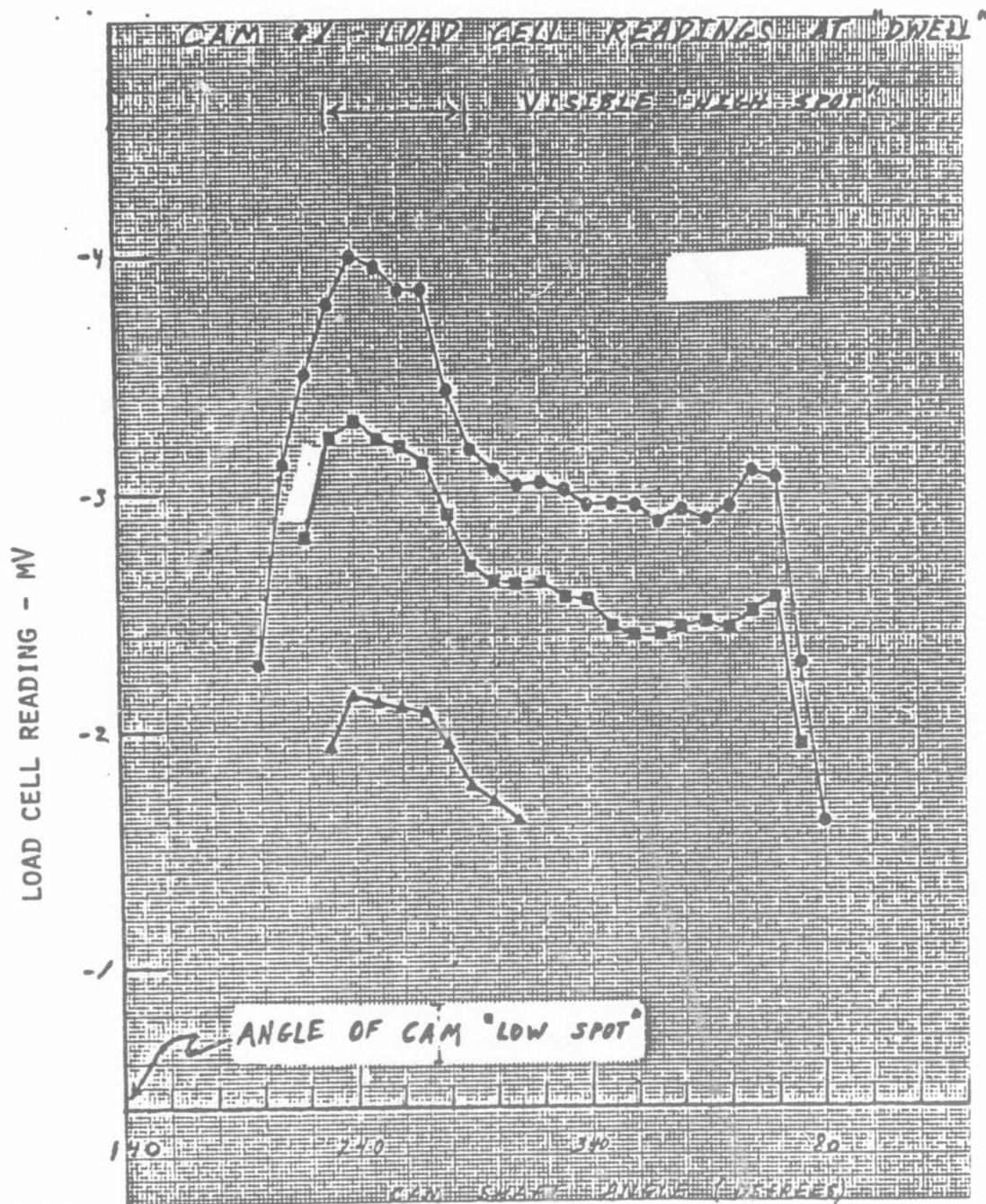


FIGURE 6. FORCE FOR NO FLOW IN CELL NO. 1 AT THREE DIFFERENT TURNBUCKLE SETTINGS

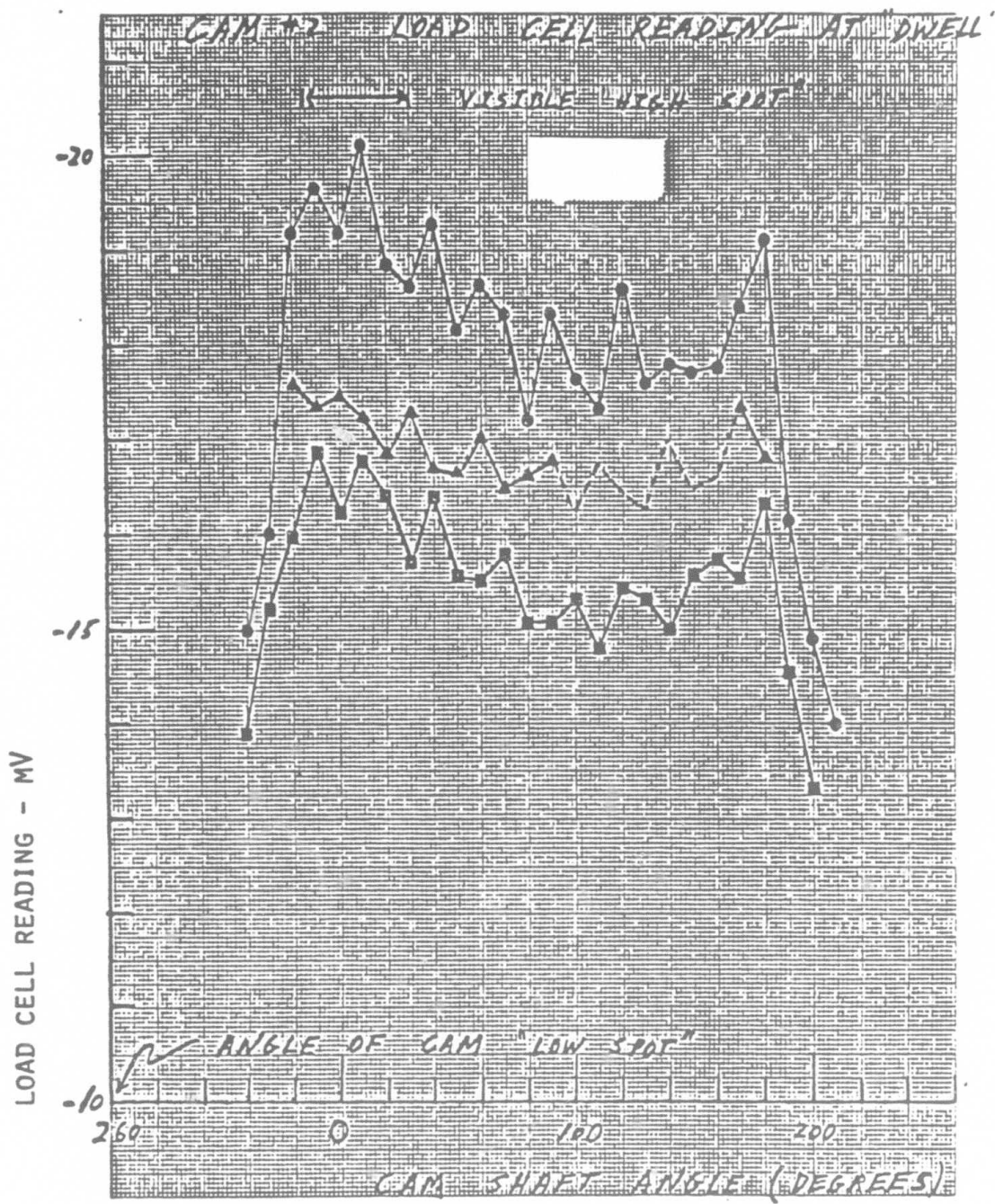


FIGURE 7. FORCE FOR NO FLOW IN CELL NO. 2 AT THREE DIFFERENT TURNBUCKLE SETTINGS

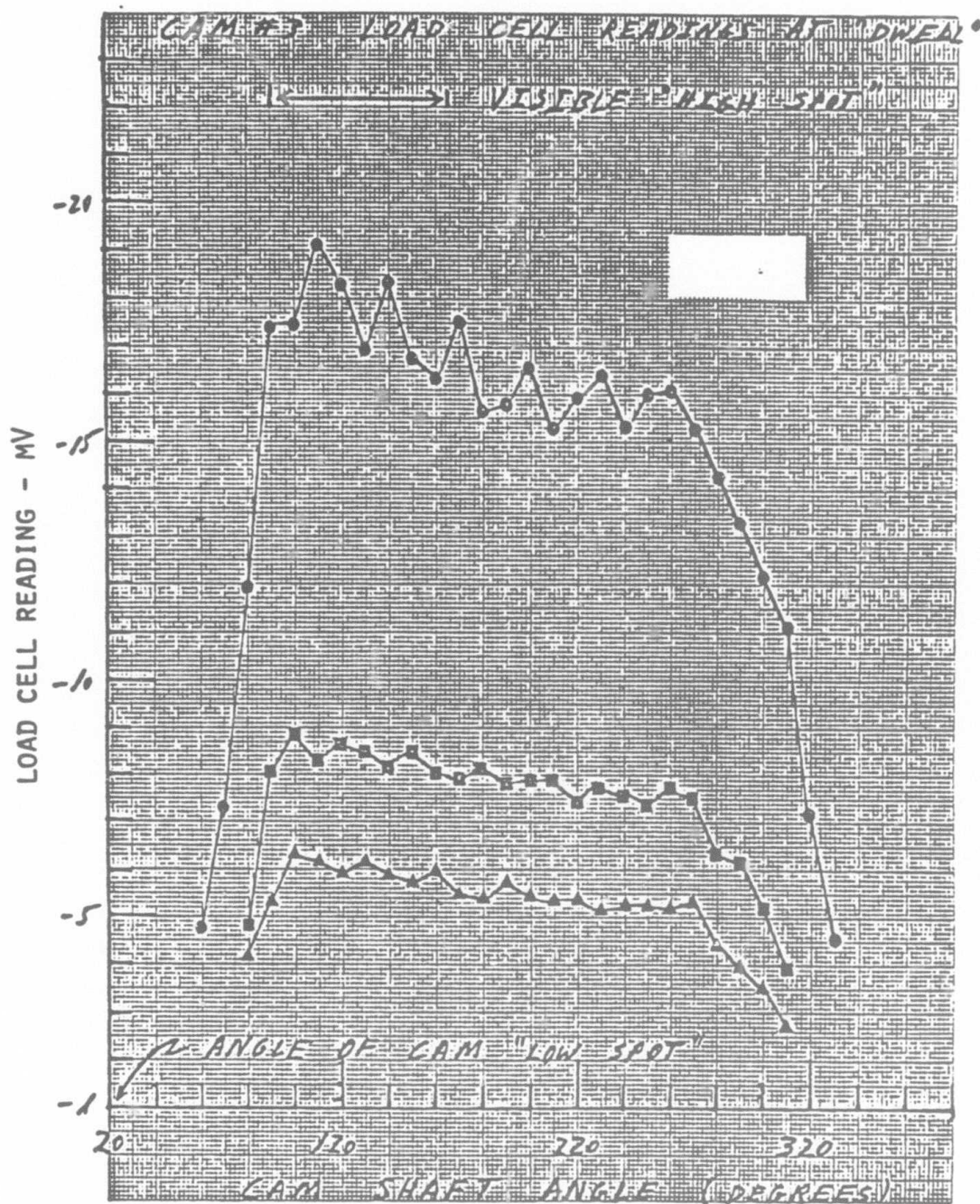


FIGURE 8. FORCE FOR NO FLOW IN CELL NO. 3 AT THREE DIFFERENT TURNBUCKLE SETTINGS

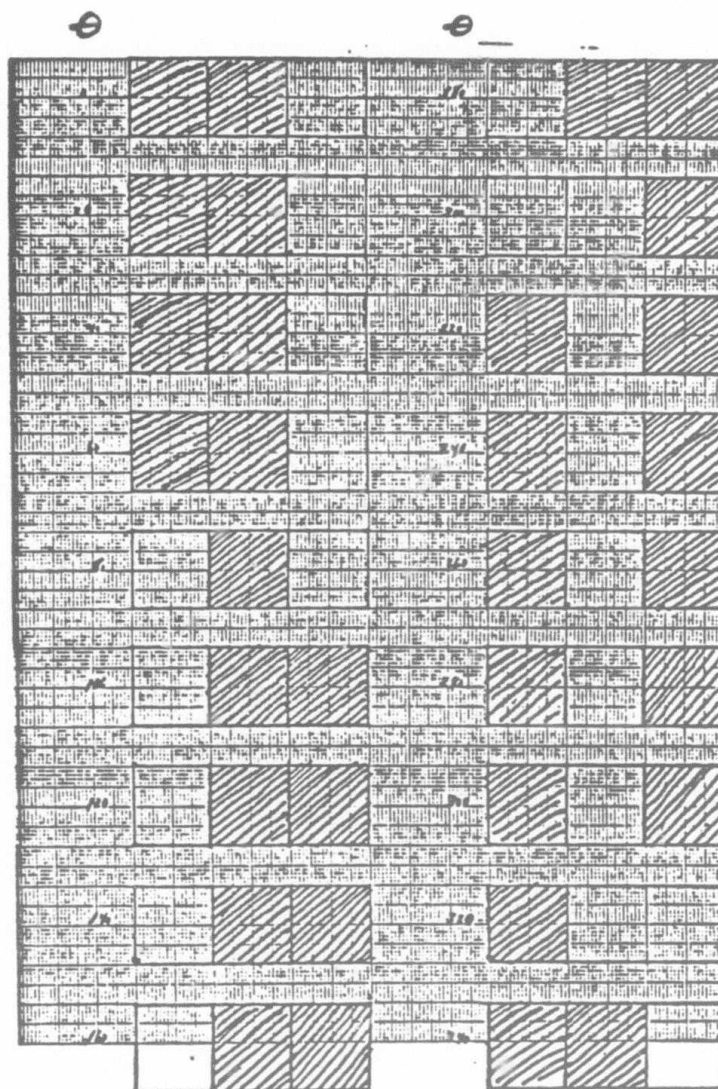


FIGURE 9. THREE CELL PHASE SEQUENCE
FOR 200° DWELL ANGLE

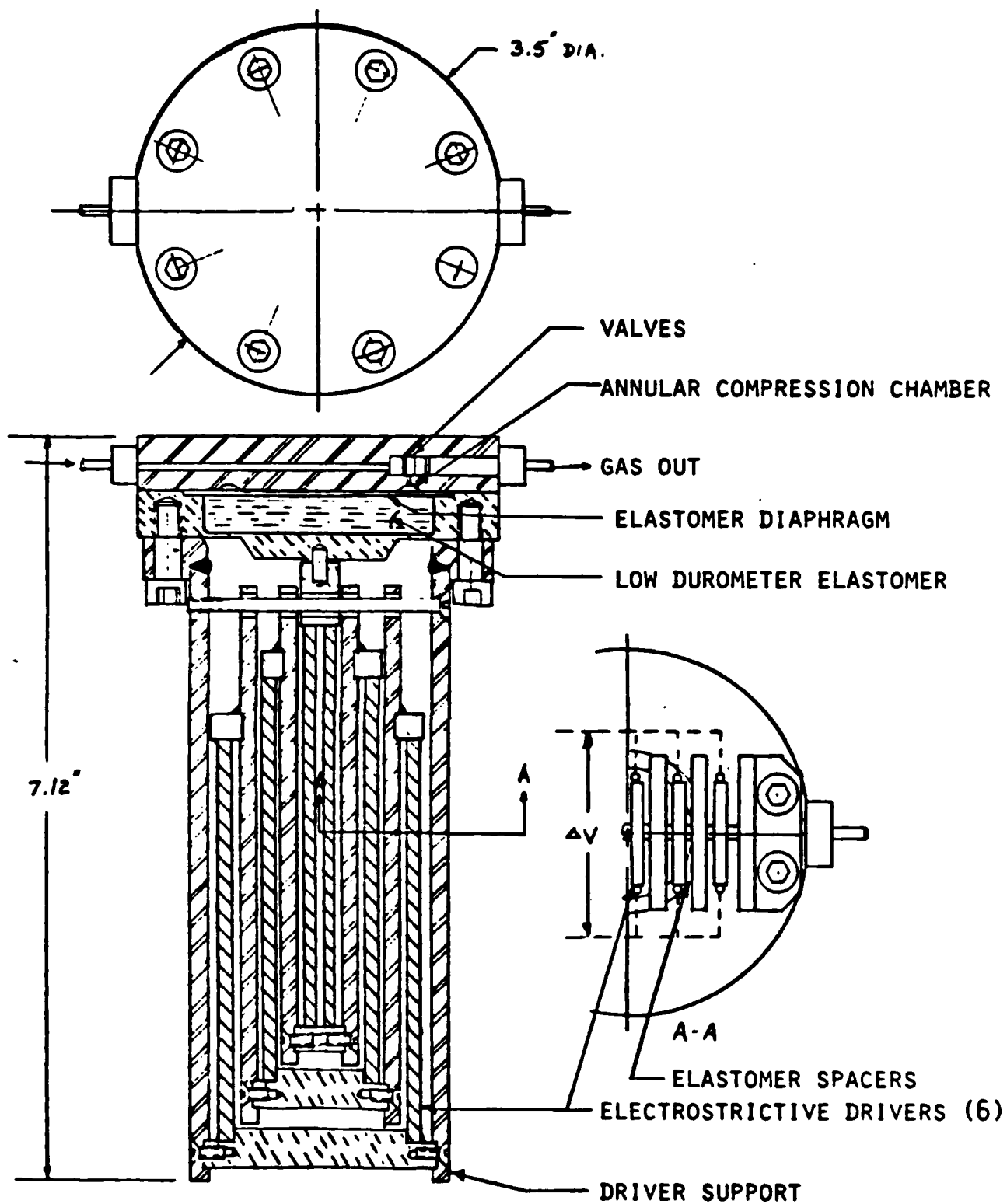


FIGURE 10. SINGLE CELL PROTOTYPE SOLID STATE COMPRESSOR

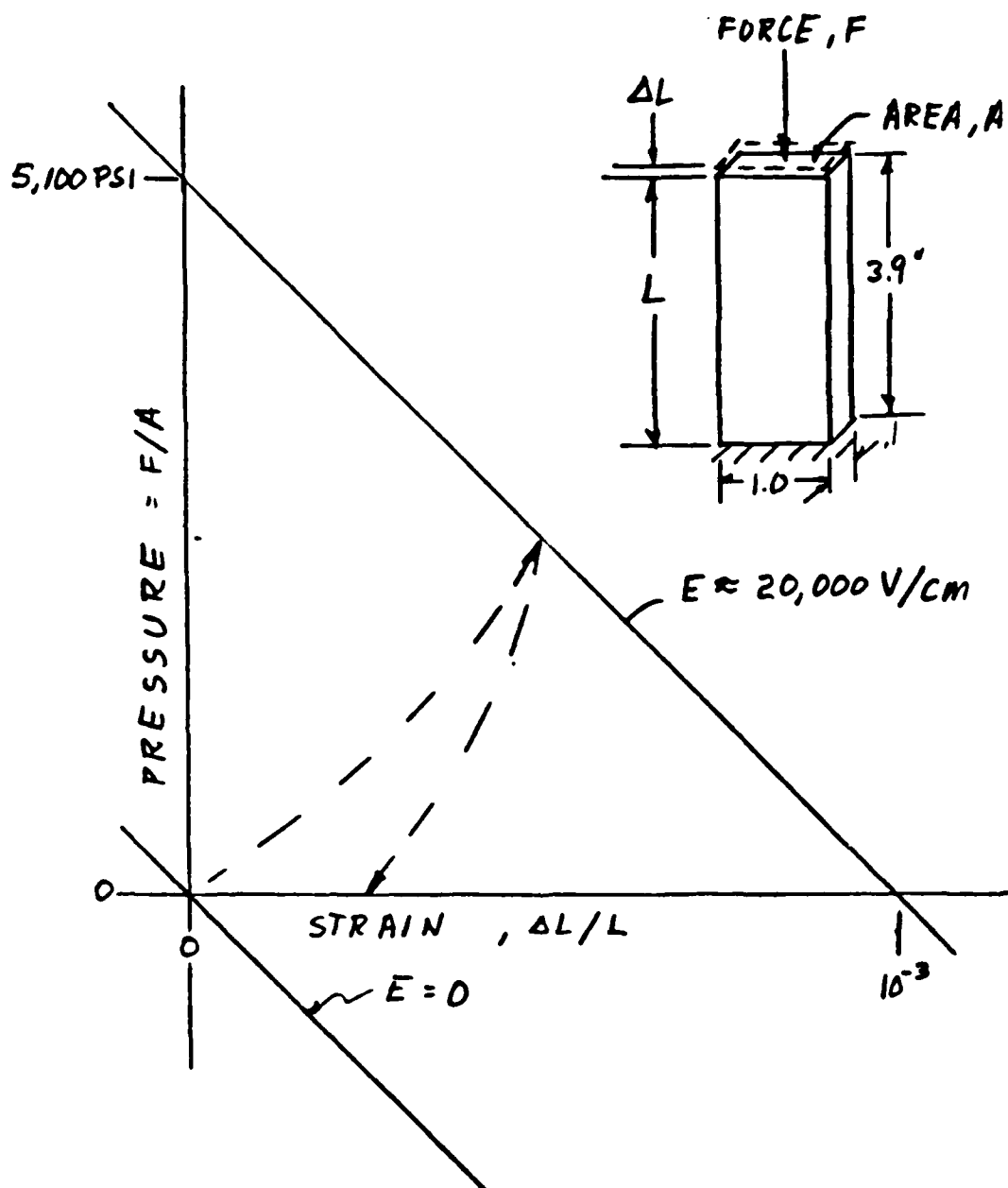


FIGURE 11. DESIGN CHARACTERISTICS OF CERAMIC DRIVERS FOR SINGLE CELL PROTOTYPE COMPRESSOR

Quarterly Report

**Development of Multilayer Electrostrictive Actuator
for Electronic Pump**

to

Air Products, Inc.

**G.O. Dayton
W.Y. Pan
G.A. DePaolis
L.E. Cross**

Appendix A

October - December 1984

1.0 INTRODUCTION

The current goals of this project are listed below.

1. To reproduce the work of Swartz and Shrout in fabricating low-pyrochlore PMN powder by the MgNb_2O_6 precursor technique and excess MgO additions.

2. To investigate the effect of MnO additions in increasing the resistivity and lowering dielectric losses in this system.

3. To develop an optimum firing schedule in terms of ceramic density, perovskite phase formation and dielectric and electrostrictive properties of sample pellets.

4. To compare multilayer devices prepared from powder prepared by Itek Optics Division with powder prepared at NRL.

5. To investigate the effects of PT addition on the electrostrictive properties of multilayer PMN devices.

6. To investigate alternative compositions in the PLZT system. Work is underway for points one through three. We are prepared to take action on point four as soon as adequate firing schedules are confirmed at which time we can begin taking data on actuators prepared at NRL.

2.0 WORK TO DATE

2.1 Raw Materials

The raw materials currently in use are listed in Table I along with values of weight loss on ignition. From this data it was decided that LOI factors could be neglected in batching raw materials for subsequent calcining.

2.2 Calcined Powders

Powders have been prepared using the calcining procedure shown in Figure

1. Compositions have been prepared with 0.000, 0.005, and 0.010 weight

percent excess MnO (added as nitrate solution), and powder with 0.050 excess is scheduled. X-ray diffraction analysis of these powders revealed significant amounts of the undesirable pyrochlore phase by the method of Swartz and Shrout where:

$$\text{pyrochlore \%} = \left[\frac{I_{\text{pyro (222)}}}{I_{\text{pyro (222)}} + I_{\text{perov (110)}}} \right] \times 100$$

The results are shown in Table II.

The powder from Itek-Optics Division was prepared following a different processing procedure which they have modified from the Swartz and Shrout technique (see Figure 2). It would appear that our powder is slightly superior to theirs on pyrochlore content alone. We have still failed to reproduce the results of Swartz and Shrout.

A sample of MgNb_2O_6 precursor powder was obtained from S.L. Swartz. It was reacted with our PbO and TiO_2 raw materials and formed a PMN 10PT with less than 3% pyrochlore. Comparison of the two MgNb_2O_6 powders revealed a darker color and a small amount of unreacted niobia in our powder. The Swartz precursor had 2 mole% excess MgO . Further checking showed that the Swartz powder was prepared from a food grade MgO (Baker Chemical #1-2480) of unknown purity and the same niobia as the present study.

On this basis we are proceeding to investigate the effects of different MgO source powders on the production of MN-precursors and PMN 10PT powders. We have on hand the high purity $\text{MgCO}_3 \cdot \text{Mg}(\text{OH})_2 \cdot n\text{H}_2\text{O}$ that we are presently using to prepare MgO . We will determine if lowering the decomposition temperature may increase the reactivity of the MgO produced since the decomposition occurs as low as 600°C .

We have also obtained food grade MgO similar to that of the earlier Swartz study and have on hand an electronic grade MgO (Fisher M-300, low activity, intermediate purity).

2.3 Fired Pellets

An attempt was made to fire pellets using a burial-source technique wherein samples are covered with coarse pre-sintered powder of the same composition in a platinum tray inside a sealed crucible. It is easy in this technique to cause fluxing of the alumina crucible by PbO-rich compounds. Since pellets of non-uniform color resulted, this method was set aside in favor of pellets on platinum sheet and PbZrO_3 filled boats in the sealed crucible as with our normal PZT firings.

A pellet study has been initiated to determine weight loss, density and electrical properties of different composition fired at 1240, 1270, and 1300°C for 60 minutes. The initial results are shown in Table III. Surprising amounts of pyrochlore were found in one of these samples. This is contrary to earlier reports that pyrochlore levels are reduced by sintering.

The room temperature electrical properties have been measured on samples from the 1240°C firing. This data is shown as a function of manganese content in Table IV. For this study, pellets were ground parallel and electroded with air dry silver. The low dielectric constant (compared to earlier work on PNN-PT) is consistent with the presence of large amounts of pyrochlore in these samples. The high losses may be due to this or to improper manganese doping.

2.4 Tape Casting

Two of the early powders prepared in this study were tape cast using our standard casting procedure. A comparison of two powder milling methods and variations in binder content shows that for good tape with reasonable green density the powder should be attritor milled for 2 or more hours after the

final calcine step and that binder contents (Cladan CB73115) near 35 weight percent will be optimum. No devices were prepared from this tape since the powder showed high pyrochlore levels.

2.5 Extrapolation of Actuator Performance to High Field Level

In simple proper ferroelectric materials such as the PMN:PT and PLZT compositions, it is expected that the dielectric behavior should be describable by Landau:Ginsburg:Devonshire phenomenology. For this approach the perturbation to the elastic Gibbs free energy, ΔG , is expanded as a power series in polarization, i.e.

$$\Delta G = \frac{1}{2} \alpha P^2 + \frac{1}{4} \beta P^4 + \frac{1}{6} \gamma P^6 \dots \quad (1)$$

since the electric field component E is given by

$$E = \frac{\partial \Delta G}{\partial P}$$

$$E = \alpha P + \beta P^3 + \gamma P^5 \dots \quad (2)$$

For the electrostrictive displacement transducer, the strain x is given by

$$x_3 = Q_{11} P_3^2 \quad (3)$$

and

$$x_1 = Q_{12} P_3^2 \quad (4)$$

Thus from the measured strain vs E it is possible to deduce directly the form of E vs P and to use equation (3) to find values for the α , β , γ , and δ . These fitted values can then be used to extrapolate to higher field level beyond the range of present measurements on bulk samples.

For a 10% PT:PMN, the longitudinal strain extrapolation is given in Figure 3; and for an 8.8:65:35 PLZT, the transverse strain extrapolation is shown in Figure 4.

3.0 CONCLUSIONS

The most important goal at this point is to develop the ability to fabricate pyrochlore-free PMN-PT powders. The condition of this powder impinges on the subsequent processing steps in terms of optimum firing procedures, studies of MnO additions and PT additions and the electrical properties of the ceramics to such a great extent that this factor cannot be overlooked. The fact that studies are proceeding in all aspects of the project means that many factors are likely to come to fruition at nearly the same time.

Figure 1. Current MRL Processing Procedure for PMN-PT Compositions.

- A.** MgO is prepared from $\text{MgCO}_3 \cdot \text{Mg}(\text{OH})_2 \cdot \text{nH}_2\text{O}$ by decomposition at 950°C , 4 hours, covered Al_2O_3 crucible.
- B.** MgNb_2O_6 is prepared by batching MgO with Nb_2O_5 in equimolar ratios. Raw oxides are attritor milled 2.5 hours in ethyl alcohol with $1/8''$ ZrO_2 media. Slurry is dried to powder at 140°C for 24 hours then hand ground in a mullite mortar and pestle for homogenization. Powder is loaded in covered ZrO_2 saggars or Al_2O_3 crucibles and calcined for 4 hours at 1000°C . The resulting cake is hand ground and stored.
- C.** PMN-PT is prepared by batching MgNb_2O_6 , PbO , TiO_2 and $\text{Mn}(\text{NO}_3)_2$ solution in proper amounts for desired compositions. These materials are ball milled for 24 hours in ethyl alcohol with $3/8''$ ZrO_2 media. The resulting slurry is dried at 140°C for 24 hours then hand ground in a mullite mortar and pestle for homogenization. Powder is loaded in covered ZrO_2 saggars or Al_2O_3 crucibles and calcined for 4 hours at 800°C . Cake is then hand ground. For pellets, the powder is ball milled, 24 hours, dried, and PVA solution is added. For tape casting powder is attritor milled 2.5 hours and mixed with Cladan CB73140 binder.

Figure 2. ITEX Processing Procedure for PMN-PT Compositions.

- A. MgNb_2O_6 powder is prepared by batching MgO (Alpha Chemical Company #88290) with 2 wt% excess, and Nb_2O_5 (Alpha #51103). The mixture is ball milled and calcined at 1030°C for 4 hours.**
- B. PMN-PT composition are prepared by batching MgNb_2O_6 + 2 Wt% MgO with PbO (National Lead Co.) and PbTiO_3 (Alpha #57107). Mixture is ball milled then calcined at 1000°C for 2 hours. Powder is ground in a mechanical mortar and pestle then recalcined at 1000°C for 2 hours. Finally, the powder is again ground in a mechanical mortar and pestle.**
- C. Parts are prepared by tape casting using Cladan binder, screen printing electrode and laminating layers. After binder burnout, devices are fired 2 hours at 1275°C on platinum mesh over PbZrO_3 (Alpha Chemical Co.) source powder.**

PMN: 10% PT

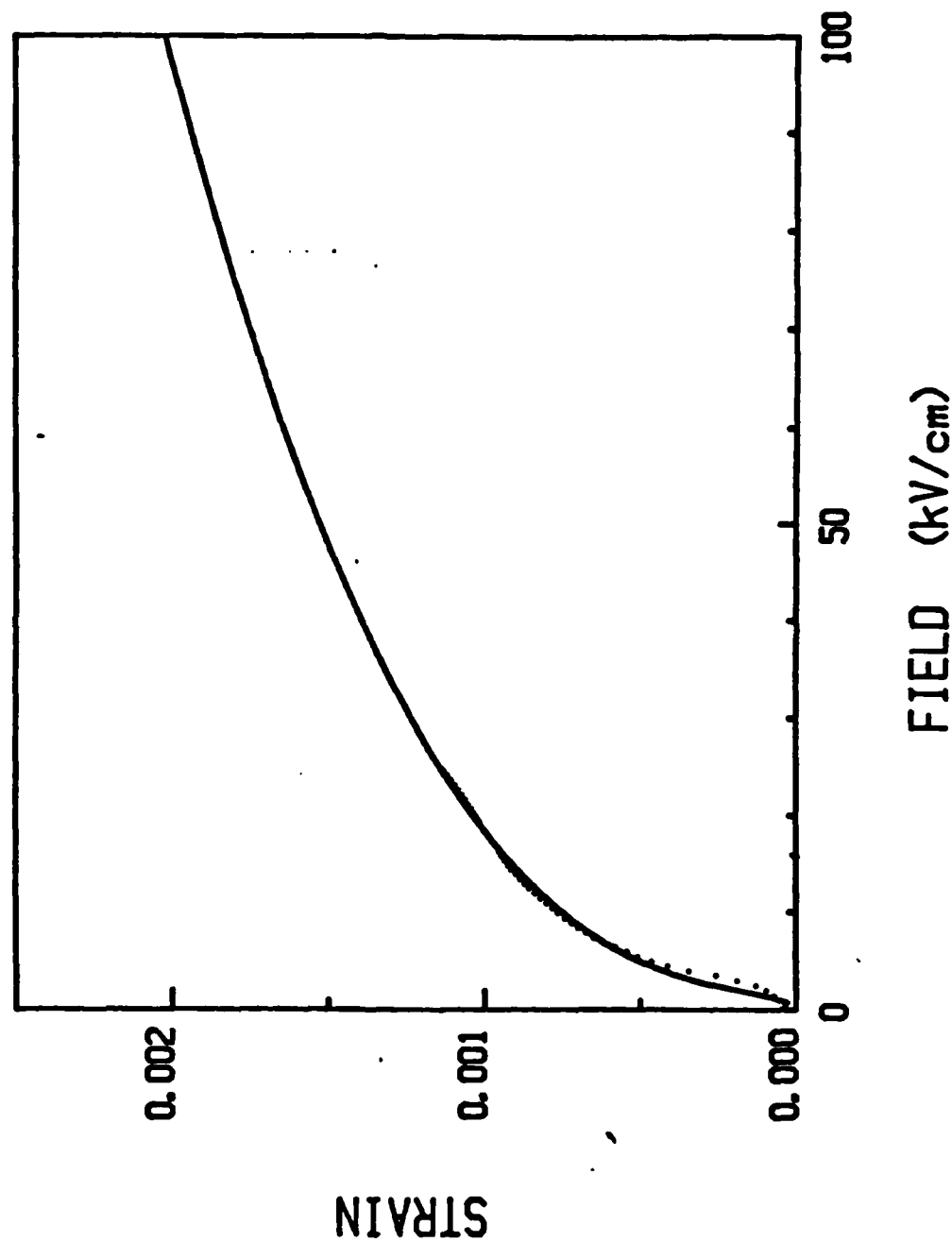


Figure 3. Longitudinal strain x_3 in PMN 10% PT.

PLZT

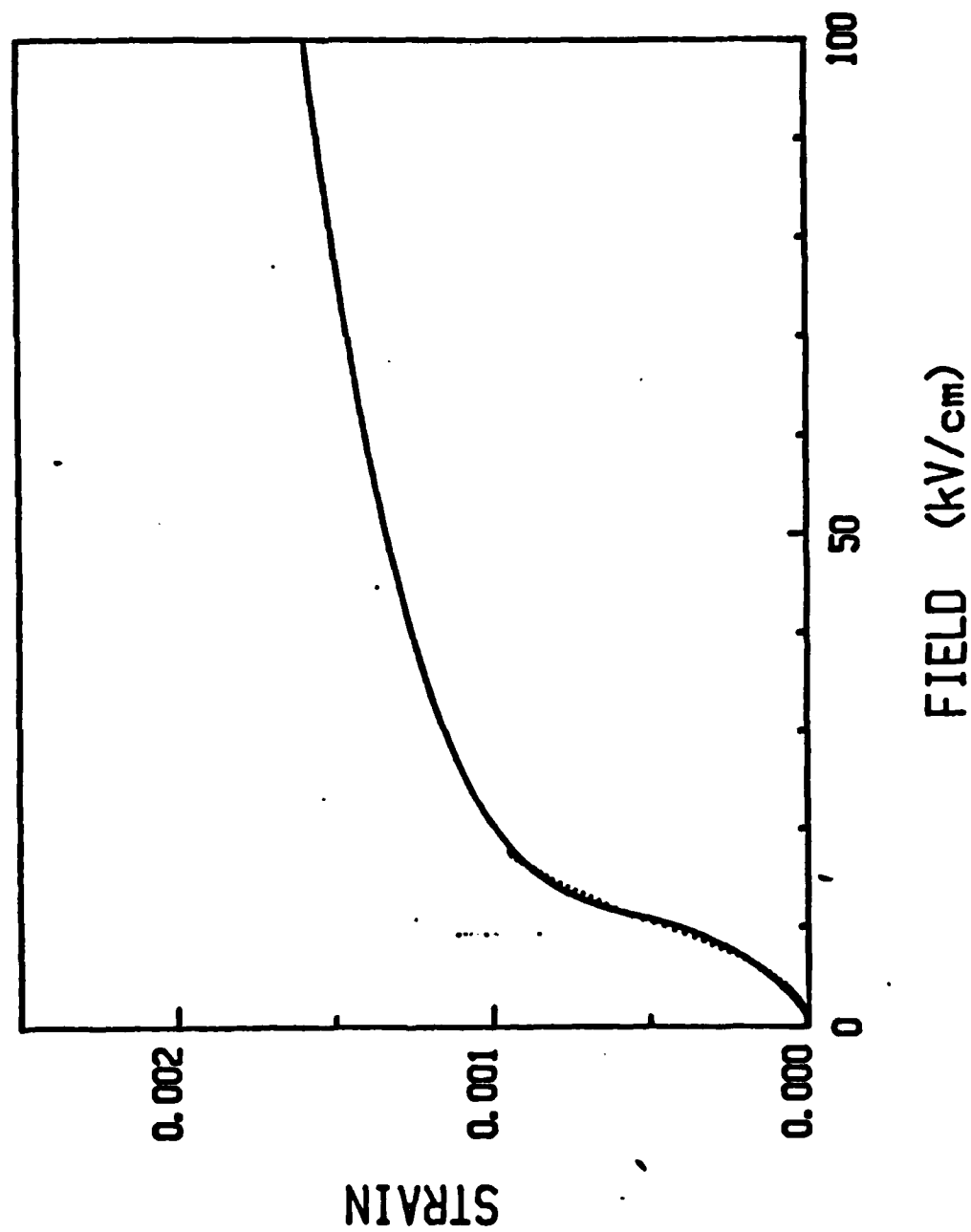


Figure 4. Transverse strain x_1 in PLZT 8.8:65:35.

Table I. Raw Materials for PMN-PT Powders.

Oxide	Loss on Ignition			Supplier Designation	Supplier
	Temp.	Time	% Wt Loss		
PbO	800°C	1 hr	0.132	100Y - Elect. Grade	Hammond Lead Product, Inc.
TiO ₂	800°C	1 hr	0.244	T-315, lot 741388	Fisher Scientific, Inc.
Nb ₂ O ₅	1000°C	1 hr	0.050	5987, lot 34	Teledyne Wah Chang-Albany
MgO	1000°C	1 hr	0.400	- see below -	
MgCO ₃ ·Mg(OH) ₂ ·nH ₂ O	950°C	4 hr	~58%	2432-5, lot 425125	J.T. Baker Chemical Co.

Table II. Pyrochlore Content of Calcined Powders.

Batch No.	MnO Conc.	% Pyrochlore
PMN 10 PT-3	0.000	11.7
PMN 10 PT-5	0.005	8.5
PMN 10 PT-4	0.010	11.7
Itek Powder (PMN 8.5 PT)	0.000	16.0
With Swartz Precursor (PMN 10 PT)	0.000	<3.0

Table III. Results of 1240°C Firing Study.

Source Powder No.	MnO Conc. wt%	Weight Loss T	<u>gm/cm³</u>	<u>% Theo.</u>	<u>% Pyrochlore</u>
PMN 10 PT-3	0.000	1.15	7.49	92.2	N.D.
PMN 10 PT-5	0.005	1.51	7.39	90.8	27%
PMN 10 PT-4	0.010	0.78	7.39	90.9	N.D.

N.D.: Not determined.

Table IV. Electrical Properties of Pellets Fired at 1240°C.

Powder No.	MnO wt%	Test Frequency					
		0.1 kHz		1.0 kHz		10 kHz	
		K	Tan δ	K	Tan δ	K	Tan δ
PMN 10 PT-3	0.000	3344	.0484	3124	.0478	2917	.0492
						2712	.0532
PMN 10 PT-5	0.005	3682	.0299	3529	.0325	3554	.0404
						3139	.0513
PMN 10 PT-4	0.010	3967	.0276	3811	.0314	3637	.0401
						3394	.0524

3-30-84
 Revised 1-1-84
 " 8-13-84
 1-8-85

DARPA TASK SCHEDULE - START 7/1/83
CONTRACT N00014-83-C-0394

